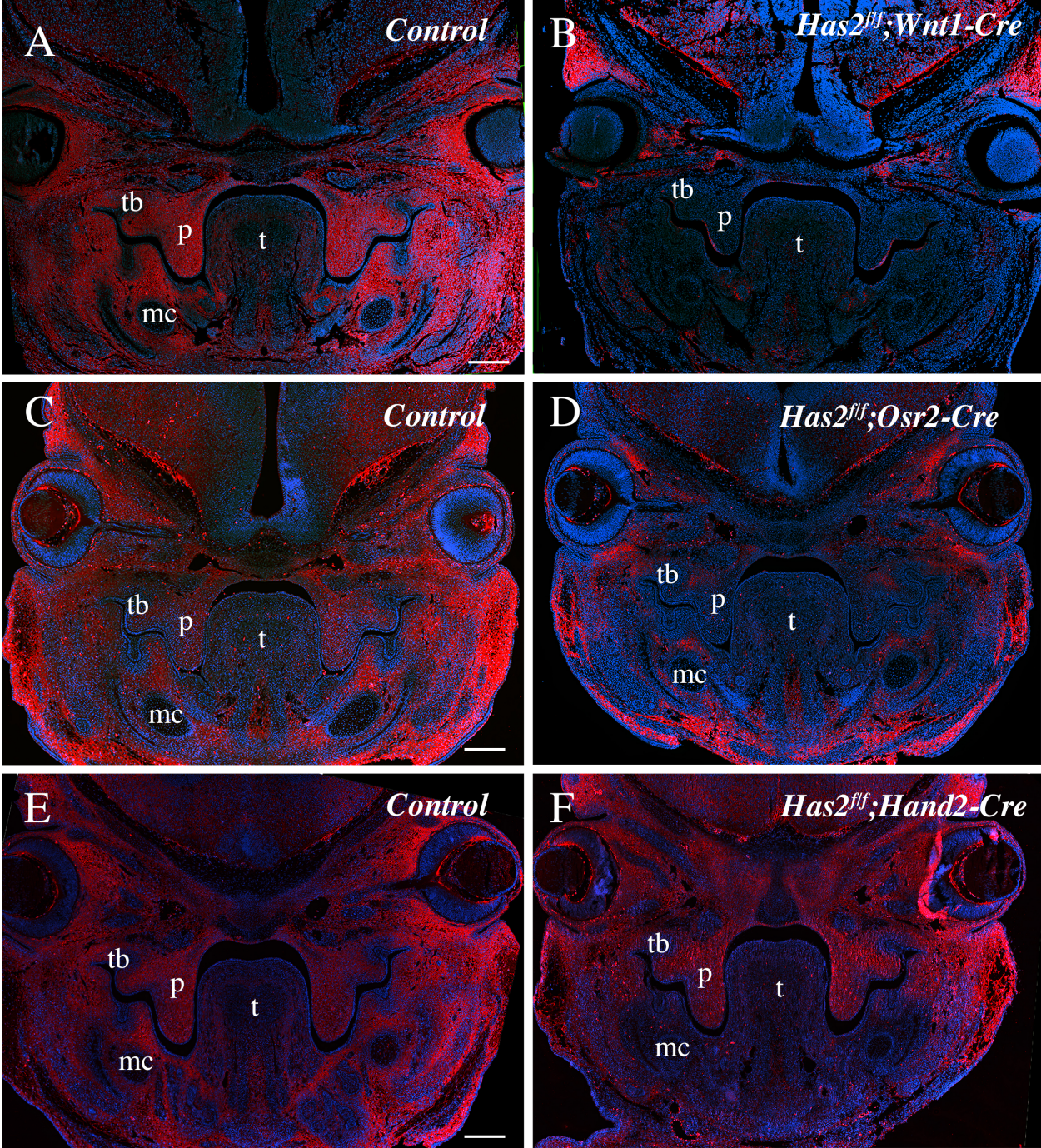
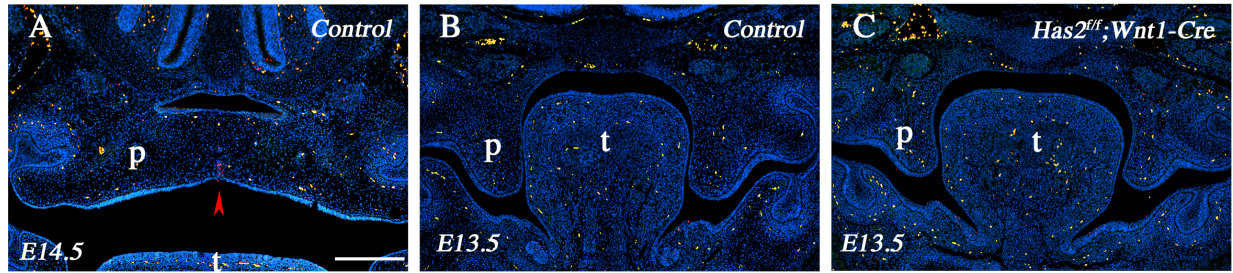


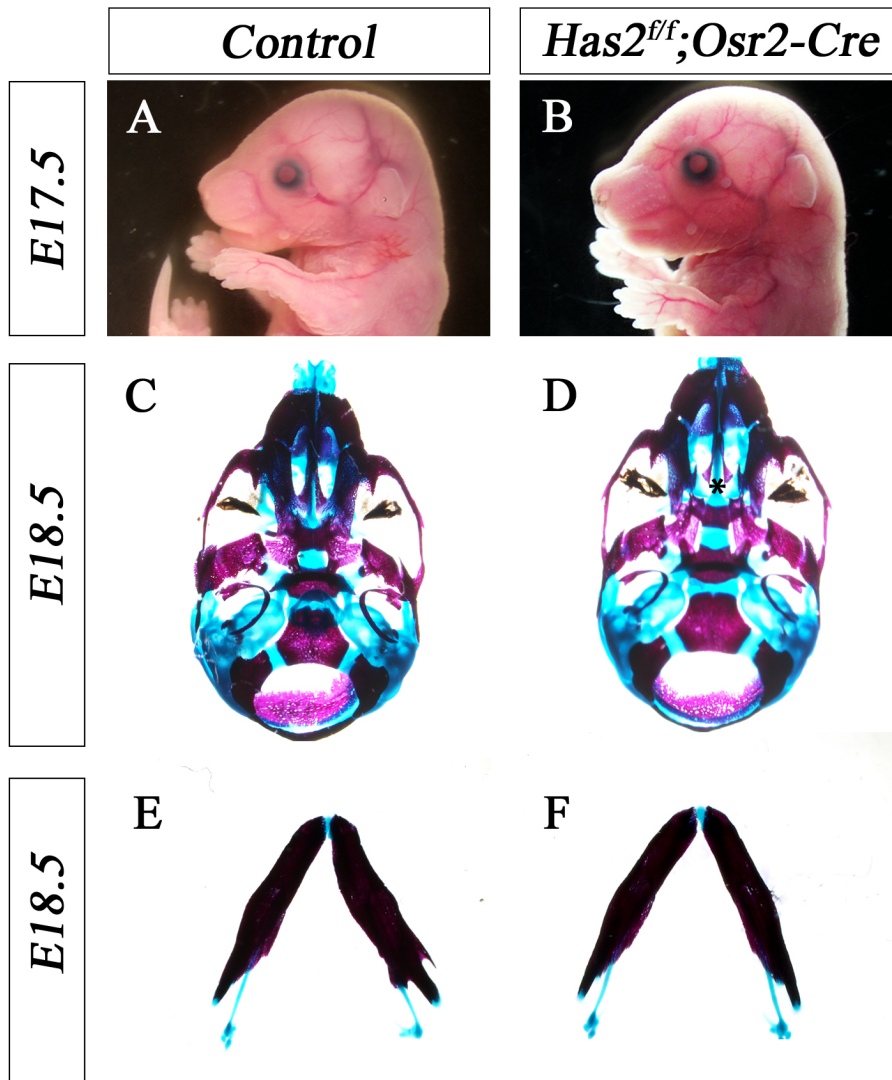
Supplementary materials for Lan et al. "Requirement of hyaluronan synthase-2 in craniofacial and palate development"



Appendix Fig. 1. Comparison of the patterns of HA accumulation and distribution in the craniofacial tissues in E13.5 *Has2* conditional mutant embryos and their control littermates detected by HABP staining. HABP bound to endogenous HA was detected in red color, with blue color showing DAPI counterstaining of cellular nuclei. (A, B) Coronal sections through the middle region of the palatal shelves of control (A) and *Has2^{ff};Wnt1-Cre* (B) embryos. Note the dramatic reduction in HA accumulation in many neural crest-derived craniofacial mesenchyme tissues, including periocular mesenchyme around the developing eyes, palatal shelf mesenchyme, maxillary and mandibular mesenchyme around the molar tooth germs, and mandibular mesenchyme around the Meckel's cartilages in the *Has2^{ff};Wnt1-Cre* mutant sample (B) in comparison with the control littermate (A). mc, Meckel's cartilage; p, palatal shelf, t, tongue, tb, tooth bud. (C, D) Coronal sections through the middle region of the palatal shelves of control (C) and *Has2^{ff};Osr2-Cre* (D) embryos. Note the highly specific reduction in HA accumulation in the palatal shelf mesenchyme, eyelid tissues, as well as maxillary and mandibular mesenchyme lingual to the molar tooth germs in the *Has2^{ff};Osr2-Cre* mutant embryo (D) compared with the control littermate (C). (E, F) Coronal sections through the middle region of the palatal shelves of control (E) and *Has2^{ff};Hand2-Cre* (F) embryos. Note the specific reduction in HA accumulation in the mandibular mesenchyme under the tongue, but not in the palatal shelves and surrounding maxillary tissues, in the *Has2^{ff};Hand2-Cre* mutant embryo (F) compared with the control littermate (E). Scale bar, 100 μ m.



Appendix Fig. 2. No aberrant apoptosis was detected in the craniofacial tissues in *Has2^{ff};Wnt1-Cre* embryos. Cells undergoing apoptosis were detected using anti-active Caspase3 antibody, with the positive immunofluorescence signal shown in red color. Scattered yellow dots show autofluorescence from blood cells. (A) A representative coronal section through the middle region of the developing secondary palate in an E14.5 wildtype embryo showing detection of active Caspase3 positive cells in the midline palatal epithelial seam (pointed by the red arrowhead). p, palatal shelf. (B, C) Coronal sections through the middle region of the palatal shelves in control (B) and *Has2^{ff};Wnt1-Cre* mutant (C) littermates stained with the same anti-active Caspase3 antibody as used for the sample shown in A. Few active Caspase3-positive cells were detected in, and no difference was observed between, the control (B) and *Has2^{ff};Wnt1-Cre* mutant (C) samples. Scale bar, 100 μ m.



Appendix Fig. 3. *Has2^{ff};Osr2-Cre* mutant mice exhibit cleft palate with no obvious defects in other craniofacial structures. (A, B) Lateral view of the heads of E17.5 control (A) and *Has2^{ff};Osr2-Cre* mutant (B) fetuses. (C, D) Palatal view of the head skeletons of E18.5 control (A) and *Has2^{ff};Osr2-Cre* mutant (B) pups. Asterisk in D mark cleft palate, with absence of palatal bone covering the cranial base. (E, F) Representative images of the mandibular skeletons of E18.5 control (E) and *Has2^{ff};Osr2-Cre* mutant (F) pups.